Research article

Zhujing Xu, Zubin Jacob and Tongcang Li*

Enhancement of rotational vacuum friction by surface photon tunneling

https://doi.org/10.1515/nanoph-2020-0391
Received July 12, 2020; accepted August 30, 2020; published online September 18, 2020

Abstract: When a neutral sphere is rotating near a surface in vacuum, it will experience a frictional torque due to quantum and thermal electromagnetic fluctuations. Such vacuum friction has attracted many interests but has been too weak to be observed. Here we investigate the vacuum frictional torque on a barium strontium titanate (BST) nanosphere near a BST surface. BST is a perovskite ferroelectric ceramic that can have large dielectric responses at GHz frequencies. At resonant rotating frequencies, the mechanical energy of motion can be converted to electromagnetic energy through resonant photon tunneling, leading to a large enhancement of the vacuum friction. The calculated vacuum frictional torques at resonances at sub-GHz and GHz frequencies are several orders larger than the minimum torque measured by an optically levitated nanorotor recently, and are thus promising to be observed experimentally. Moreover, we calculate the vacuum friction on a rotating sphere near a layered surface for the first time. By optimizing the thickness of the thin-film coating, the frictional torque can be further enhanced by several times.

***Corresponding author: Tongcang Li**, Department of Physics and Astronomy, Purdue University, West Lafayette, IN 47907, USA; School of Electrical and Computer Engineering, Purdue University, West Lafayette, IN 47907, USA; Purdue Quantum Science and Engineering Institute, Purdue University, West Lafayette, IN 47907, USA; and Birck Nanotechnology Center, Purdue University, West Lafayette, IN 47907, USA, E-mail: tcli@purdue.edu. https://orcid.org/0000-0003-3308-8718
Zhujing Xu, Department of Physics and Astronomy, Purdue University, West Lafayette, IN 47907, USA. https://orcid.org/0000-0003-1780-9132
Zubin Jacob, School of Electrical and Computer Engineering, Purdue University, West Lafayette, IN 47907, USA; Purdue Quantum Science and Engineering Institute, Purdue University, West Lafayette, IN 47907, USA; and Birck Nanotechnology Center, Purdue University, West Lafayette, IN 47907, USA

Keywords: optical levitation; perovskite materials; surface photon tunneling; vacuum friction.

1 Introduction

Quantum fluctuations of electromagnetic fields cause an attractive force between two neutral metallic plates, which was first calculated in 1948 and well known as Casimir force [1]. Besides the Casimir force between static macroscopic objects, the fluctuating electromagnetic fields can cause noncontact vacuum friction between two surfaces in relative motion [2, 3]. Many efforts have been made for studying the vacuum friction between various materials and configurations [4–10]. However, former attempts using atomic force microscopes had not successfully detected the vacuum friction [11–13]. The difficulty mainly comes from the small value of vacuum friction. It is thus worthwhile to understand the mechanisms of vacuum friction better and look for enhancements of the vacuum friction. At the same time, it is essential to develop a suitable ultrasensitive detector for the measurement.

In this letter, we investigate the vacuum friction on a rotating nanosphere levitated near a flat plate (Figure 1(a)), inspired by recent breakthroughs in levitated optomechanics. There are growing interests in using optically levitated dielectric particles in vacuum for precision measurements since they are well isolated from the environment and have ultrahigh sensitivity [14–21]. Microspheres and nanospheres have been optically levitated near surfaces [22, 23]. Meanwhile, levitated nanoparticles have been driven to rotate up to 5 GHz by a circularly polarized laser [19]. Remarkably, a rotating nanoparticle levitated at 10^{-5} torr has measured a torque as small as 5×10^{-28} Nm in just 100 s [19].

Similar to the vacuum frictional force between two plates that have relative motions [2, 3], there will be a vacuum frictional torque on a nanosphere rotating at a high speed [6, 10]. Thus a levitated nanorotor provides a promising method to detect the vacuum frictional torque. Former calculations have found that the vacuum frictional torque on a 150 nm-diameter silica nanosphere near a silica

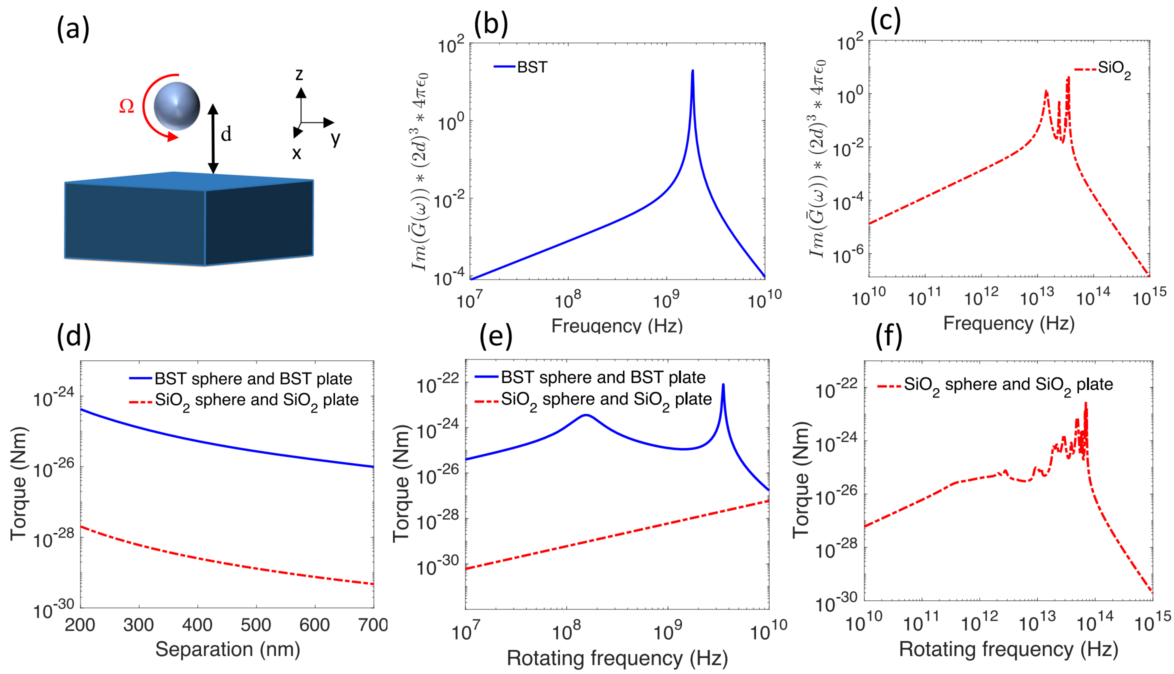

Figure 1: Vacuum friction between a rotating nanosphere and a substrate.
(a) A sphere with a radius of 75 nm rotates around the *x* axis. The *z* axis is normal to the substrate. (b) The imaginary part of the Green function (Eq. (3)) between a barium strontium titanate (BST) substrate and a nearby nanosphere. (c) The imaginary part of the Green function between a SiO_2 substrate and a nearby nanosphere. (d) Calculated vacuum friction torque acting on a BST/silica nanosphere near a BST/silica surface as a function of the separation between the sphere and the substrate. The sphere rotates at a frequency of 150 MHz, which is a resonant frequency of BST. (e) The frictional torque on a BST/silica sphere near a BST/silica surface is shown as a function of the rotating frequency of the nanosphere. The separation between the sphere and the substrate is 300 nm. (f) The friction torque of a SiO_2 sphere near a SiO_2 surface is shown at a higher frequency range. The separation is 300 nm.

surface is about 6×10^{-29} Nm at a separation of 300 nm when the sphere is rotating at 1 GHz and both the surface and the sphere are at a temperature of 300 K [19]. To measure the vacuum friction between a silica sphere and a silica plate, the experiment needs to be conducted under ultrahigh vacuum below 10^{-9} torr [19]. In this work, we propose to use BST, which is a perovskite ferroelectric ceramic that can have a large dielectric resonance at GHz frequency [24], to dramatically enhance the vacuum friction by resonant surface photon tunneling at sub-GHz and GHz frequencies. We show that the vacuum frictional torque on a BST sphere near a BST plate can be significantly enhanced to 3.6×10^{-24} Nm and 8.1×10^{-23} Nm through resonant photon tunneling at a rotating frequency of 150 MHz and 3.5 GHz, respectively. So the torque on a BST sphere near a BST plate can be measured at a pressure of about 10^{-4} torr.

The enhancement of the vacuum friction comes from photon tunneling between two surfaces. At the resonant condition, the conversion of the mechanical energy of motion to the electromagnetic energy is realized efficiently. In the domain of the rotation frequency, there are two resonances that correspond to the normal and anomalous Doppler effect [25–27]. The resonant tunneling occurs when the mechanical rotation frequency matches the sum or the difference of the surface plasmon or phonon polariton frequencies. For metals and semiconductors, the surface plasmon or phonon polariton frequency is usually on the order of 10^{14} Hz and 10^{12} Hz, respectively. Such a high surface polariton frequency makes it extremely difficult to experimentally reach the resonant condition [25–27]. Here we choose a ferroelectric material BST which has low surface polariton frequency at GHz range [24]. The dielectric properties of BST can also be tuned by fabrication and doping. When the mechanical rotating frequency of the sphere is also around GHz, the vacuum frictional torque can be significantly enhanced due to the resonant photon tunneling. In this way, the vacuum frictional torque is several orders higher than the minimum detectable torque. Besides the huge enhancement, for the first time we will show the vacuum friction between a BST sphere and a multilayer coating on top of a BST substrate. The torque can be further increased by several times by optimizing the thickness of the coating layer.

This paper is organized as follows. We show the general method of calculating the vacuum frictional torque on a rotating nanosphere and discuss the condition for the resonant photon tunneling in Section 2. The calculated friction torque acting on a BST sphere near a BST plate is presented in Section 3. In this section, we show a significant enhancement of the friction torque. Section 4 is devoted to showing the torque on a BST sphere near a multilayer coating on top of a BST substrate. The transfer matrix for calculating the optical matrix of the multilayer structure is introduced. Further enhancement of the friction torque is demonstrated.

2 Resonances in a rotating nanosphere near a surface

As a ferroelectric material, BST possesses many exceptional dielectric properties such as high dielectric constant, low loss and large electric-field dielectric tunability over a wide frequency range [24]. Especially, it has low surface polariton frequency which is favorable for enhancing the vacuum friction torque at sub-GHz and GHz frequencies.

We investigate on a case that a sphere with radius r is rotating with frequency Ω in vacuum and is placed at a separation of d from the substrate as shown in Figure 1(a). We work within the nonrelativistic and near-field limit. Thus the separation needs to be far smaller than both c/Ω (≈5 cm at 1 GHz) and $c\hbar/k_B T_j$ (≈8 μm at 300 K). Besides, the dipole approximation requires the radius of the nanosphere to be sufficiently smaller than the separation. The friction torque experienced by the sphere is written as [10].

$$M_p = -\frac{2\hbar}{\pi}\int_{-\infty}^{\infty}[n_1(\omega-\Omega)-n_0(\omega)] \times \mathrm{Im}[\alpha(\omega-\Omega)]\mathrm{Im}\left[\overline{G}(\omega)\right]d\omega \tag{1}$$

where $n_j(T) = [\exp(\hbar\omega/k_B T_j) - 1]^{-1}$ is the Bose–Einstein distribution function at temperature T_j and $j = 0, 1$ are for the substrate and the sphere, respectively. $\alpha(\omega)$ is the electric polarizability of the nanosphere. $\overline{G}(\omega)$ is the Green function such that $\overline{G}(\omega) = [G_{yy}(\omega) + G_{zz}(\omega)]/2$, where G_{yy} and G_{zz} are electromagnetic Green tensor components and x is the axis of the rotation. The polarizability and the Green function can be described as

$$\alpha(\omega) = 4\pi\epsilon_0 R^3 \frac{\epsilon_{\mathrm{sp}}(\omega)-1}{\epsilon_{\mathrm{sp}}(\omega)+2}, \tag{2}$$

$$\overline{G}(\omega) = \frac{3}{8\pi\epsilon_0(2d)^3}\frac{\epsilon_{\mathrm{sub}}(\omega)-1}{\epsilon_{\mathrm{sub}}(\omega)+1}, \tag{3}$$

where ϵ_{sp} and ϵ_{sub} are the dielectric functions of the sphere and the substrate, respectively. The equations above are for the situation that the rotation axis of the sphere is parallel to the substrate surface. When the rotating axis is normal to the surface, the Green function has a factor of $\frac{2}{3}$ difference and hence the friction torque is [28].

$$M_n = \frac{2}{3}M_p, \tag{4}$$

where M_n and M_p stand for the torque when the sphere is rotating normal and parallel to the surface, respectively. Notice that all the following calculations of the vacuum frictional torque are for the parallel case. As we can see, the friction torque depends on the optical properties of the interacting materials. The dielectric functions of different dielectric materials can be modeled as Lorentz oscillators, which treat each discrete vibrational mode as a classical damped harmonic oscillator:

$$\epsilon(\omega) = \epsilon_\infty\left(1+\sum\frac{\omega_L^2-\omega_T^2}{\omega_T^2-\omega^2-i\Gamma\omega}\right), \tag{5}$$

where ϵ_∞ is the permittivity in the high-frequency limit, ω_L is the longitudinal polar-optic phonon frequency, ω_T is the transverse polar-optic phonon frequency and γ is the damping coefficient.

As mentioned above, we are looking at the resonant photon tunneling between surface phonon polaritons to realize enhancement of the vacuum friction. Similar to the normal and anomalous Doppler effect for the system of two sliding plates [25–27], rotational friction between a rotating sphere and a flat plate also has such resonances. BST is a good candidate for realizing such resonant photon tunneling since it can support low-frequency surface polariton modes. The optical phonon parameters of BST are $\epsilon_\infty = 2.896$, $\omega_L = 1.3\times10^{10}\ \mathrm{s}^{-1}$, $\omega_T = 5.7\times10^{9}\ \mathrm{s}^{-1}$, $\Gamma = 2.8\times10^{8}\ \mathrm{s}^{-1}$ [24].

The friction increases significantly at the rotating frequency $\Omega = |\omega_{1p} \pm \omega_{2p}|$ which correspond to the resonant generation of surface polaritons. Here Ω is the rotating frequency of the sphere. ω_{1p} and ω_{2p} are surface polariton frequencies such that $\mathrm{Re}(\epsilon(\omega_{1p})) = -2$ and $\mathrm{Re}(\epsilon(\omega_{2p})) = -1$, which lead to large $\alpha(\omega)$ and $\overline{G}(\omega)$. Two resonant frequencies are $\omega_{1p} = 1.06\times10^{10}\ \mathrm{s}^{-1}$ and $\omega_{2p} = 1.15\times10^{10}\ \mathrm{s}^{-1}$. Therefore, when the rotation frequency $\Omega = |\omega_1 - \omega_2| = 2\pi\times150\,\mathrm{MHz}$ or $\Omega = \omega_1 + \omega_2 = 2\pi\times3.52\,\mathrm{GHz}$, the friction will be greatly enhanced. Figure 1(b) shows the Green function that connects the dipole moment fluctuation of the sphere and the induced electromagnetic field on a BST surface. As a comparison, the Green function for a silica surface is presented in Figure 1(c). The frequency of surface polaritons for a silica surface [29] is around 10^{13} Hz, which is several orders higher than the frequency of BST. To meet the condition of resonant photon tunneling between a silica sphere and a silica plate, the rotation frequency of the sphere will need to reach 10^{13} Hz which cannot be achieved experimentally.

3 Vacuum friction between a BST nanosphere and a BST plate

The calculated vacuum friction between a BST sphere and a BST plate is presented in this section. Here, we investigate on a case that the radius of the sphere is 75 nm [19] and the sphere and the plate have the same temperature of 300 K. At a separation of 300 nm, the calculated friction torque is shown as a function of rotating frequency in Figure 1(e). The blue solid curve corresponds to the friction between a BST sphere and a BST plate. It shows two resonant peaks of the torque at 150 MHz and 3.52 GHz as expected before. The amplitude of the friction torque at two resonant frequencies are several orders higher than the nonresonant part. The maximum torque of 8.06×10^{-23} Nm is achieved at 3.52 GHz. The red dashed curve is the friction torque acting on a silica sphere near a silica plate, for comparison. The low-frequency surface polariton mode and resonant photon tunneling significantly enhance the amplitude of the vacuum friction. At 150 MHz and 3.52 GHz, the friction torque between a BST sphere and a BST surface has an enhancement of about 4×10^5 compared to the torque between a silica sphere and a silica surface.

Figure 1(f) shows the calculated torque for silica at much higher rotation frequencies. Similarly, silica also has resonant photon tunneling conditions and at such frequencies, the torque can also be greatly enhanced. At a rotating frequency of around 100 THz, the torque can also be near 10^{-22} Nm. However, this frequency is far beyond the current experimental limit. The calculated friction torque as a function of the separation between the sphere and the substrate is shown in Figure 1(d) at a rotating frequency of 150 MHz, which is the resonant frequency of BST. For each separation, the enhancement is more than five orders.

A recent experiment has detected a torque of 5×10^{-28} Nm with an optically levitated nanosphere at 10^{-5} torr [19]. It is four orders smaller than the vacuum frictional torque on a BST sphere at resonant frequency. Another factor that can affect the detection of vacuum friction is the air damping torque. The air damping torque on a rotating nanosphere due to residual air molecules in the vacuum chamber can be described as [30]:

$$M_{\text{air}} = \frac{\pi p \Omega (2r)^4}{11.976} \sqrt{\frac{2m_{\text{gas}}}{\pi k_B T}}, \tag{6}$$

where p is the air pressure, r is the sphere radius, $m_{\text{gas}} = 4.8 \times 10^{-26}$ kg is the mass of the air molecule and T is the temperature of the surrounding air molecules. At the pressure of 10^{-4} torr, the air damping torque acting on the sphere is 4.5×10^{-24} Nm at a rotating frequency of 150 MHz at room temperature, which is about one orders smaller than the targeted vacuum friction torque. 10^{-4} torr and lower pressures have been achieved in levitation experiments [19, 31]. Compared to silica, the requirement of pressure for measuring vacuum friction on a BST nanosphere is substantially relaxed.

4 Effects of surface coating

We have demonstrated the vacuum friction between a BST sphere and a BST plate and showed that the friction can be enhanced by several orders due to the surface resonant photon tunneling. It will be easier to experimentally realize this condition when the resonant frequency is as low as possible. In this section we show that the resonant frequency can be lowered by thin-film coating.

We investigate on the friction torque on a BST sphere near a surface that has a thin layer of dielectric coating on top of a BST substrate as shown in Figure 2(a). To calculate the vacuum frictional torque, we need to get the reflection coefficients for the layered structure by the transfer matrix method. For a surface that has a thin layer on top of a substrate, the transfer matrix for the $p(s)$ polarization is given as [32, 33]

$$T^{p(s)} = D^{p(s)}_{0\to1} P(L_1) D^{p(s)}_{1\to2}, \tag{7}$$

where L_1 is the thickness of the thin layer. Here $j = 0, 1, 2$ stands for the vacuum between the sphere and the surface, the thin layer, and the BST substrate, respectively. $D^{p(s)}_{j,j+1}$ is the transmission matrix between layer j and j+1 for the $p(s)$ polarization and it can be written as

$$D^{p(s)}_{j\to j+1} = \frac{1}{2}\begin{bmatrix} 1+\eta^{p(s)}_{j,j+1} & 1-\eta^{p(s)}_{j,j+1} \\ 1-\eta^{p(s)}_{j,j+1} & 1+\eta^{p(s)}_{j,j+1} \end{bmatrix}, \tag{8}$$

where $\eta^{p(s)}_{j,j+1}$ is given as

$$\eta^{p}_{j,j+1} = \frac{\epsilon_j k_{j+1,z}}{\epsilon_{j+1} k_{j,z}}, \quad \eta^{s}_{j,j+1} = \frac{k_{j+1,z}}{k_{j,z}}. \tag{9}$$

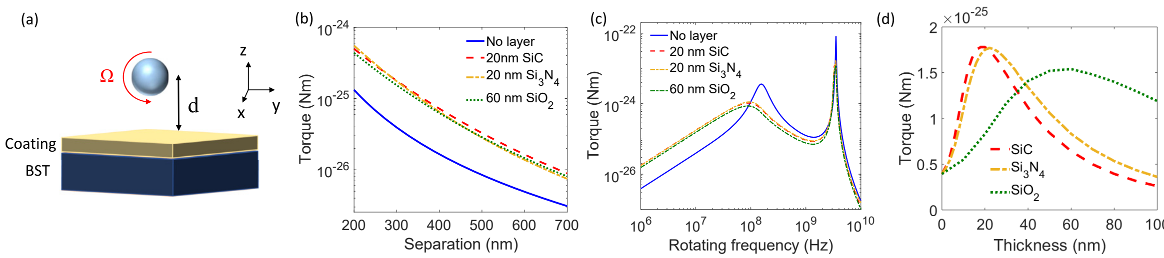

Figure 2: Vacuum friction between a barium strontium titanate (BST) sphere and a BST substrate with a single-layer coating. (a) A sphere with a radius of 75 nm rotates around the *x* axis. The *z* axis is the direction normal to the substrate. The plate consists of a thin layer of dielectric material (shown in yellow) and a BST substrate (shown in blue). (b) Calculated vacuum frictional torque acting on the nanosphere as a function of the separation between the sphere and the substrate. The sphere rotates at a frequency of 10 MHz. The red, yellow, and green dashed curve correspond to the case for a 20-nm SiC, 20-nm Si_3N_4, and a 60-nm SiO_2 thin layer. The blue solid curve is for the case when there is no coating. (c) The frictional torque is shown as a function of the rotating frequency of the nanosphere. The separation is 300 nm. The blue solid curve shows the case when there is no coating on the BST substrate. The red, yellow, and green dashed curve correspond to the case for a 20-nm SiC, a 20-nm Si_3N_4, and a 60-nm SiO_2 thin layer on top of the BST substrate. (d) The frictional torque is shown as a function of the thickness of the thin layer on top of the BST substrate for the case of SiC, Si_3N_4, and SiO_2. Here the separation is 300 nm and the rotating frequency is 10 MHz.

Here $k_{j,z} = \sqrt{\epsilon\omega^2/c^2 - k_\parallel^2}$ is the vertical wave vector for the jth layer. $k_\parallel$ is the wave vector parallel to the surface. $P(L_j)$ is the propagation matrix in the jth layer for both p and s polarizations and it is given as

$$P(L_j) = \begin{bmatrix} e^{-ik_{j,z}L_j} & 0 \\ 0 & e^{ik_{j,z}L_j} \end{bmatrix}. \tag{10}$$

With the transfer matrix M, the optical properties such as reflection, transmission and absorption for the layered structure can be calculated. The reflection coefficients for the $p(s)$ polarization of the layered structure is [32, 33].

$$r_{p(s)} = T_{21}^{p(s)} / T_{11}^{p(s)}. \tag{11}$$

where $T_{21}^{p(s)}$ and $T_{21}^{p(s)}$ are the components of the transfer matrix T. To calculate the vacuum friction between a sphere and a layered structure, we need to get the electromagnetic Green tensor and it is given as [34]

$$G(\omega) = i\int_0^\infty dk_\parallel k_\parallel e^{2ik_z d} \cdot \left[r_p(\omega, k_\parallel) \begin{pmatrix} -k_z/2 & 0 & 0 \\ 0 & -k_z/2 & 0 \\ 0 & 0 & k_\parallel^2/k_z \end{pmatrix} + r_s(\omega, k_\parallel) \begin{pmatrix} k^2/2k_z & 0 & 0 \\ 0 & k^2/2k_z & 0 \\ 0 & 0 & 0 \end{pmatrix} \right], \tag{12}$$

where d is the separation between the sphere and plate, $k = \omega/c$ is the total wave vector, $k_\parallel$ is the wave vector parallel to the surface, $k_z = \sqrt{k^2 - k_\parallel^2}$ is the wave vector perpendicular to the surface. r_s and r_p are the reflection coefficients of the layered structure which have been calculated by the transfer matrix. Therefore, the Green function that associates the dipole moment fluctuations of the sphere and the induced electromagnetic field on the layered surface is given as

$$\begin{aligned} \overline{G}(\omega) &= \frac{1}{2}(G_{yy} + G_{zz}) \\ &= \frac{i}{2}\int_0^\infty dk_\parallel k_\parallel e^{2ik_z d} \left[-r_p(\omega, k_\parallel)\frac{k_z}{2} \right. \\ &\quad \left. + r_s(\omega, k_\parallel)\frac{k^2}{2k_z} + r_p(\omega, k_\parallel)\frac{k_\parallel^2}{k_z} \right]. \end{aligned} \tag{13}$$

Based on the transfer matrix introduced above, now we can calculate the friction torque experienced by a sphere near a layered structure as shown in Figure 2(a). At a rotating frequency of 10 MHz, the calculated friction as a function of the separation is shown in Figure 2(b). The red, yellow, and green dashed curve is the case for a single layer of 20-nm SiC, 20-nm Si_3N_4, and 60-nm SiO_2 on top of the BST. The blue solid curve is the case for a BST sphere and a BST substrate, for comparison. The optical properties of SiC, Si_3N_4, and SiO_2 can be found in [29, 34]. We can see that the torque for the single-layer coating is enhanced by about four times compared to the no-coating case. We also show the calculated friction as a function of the rotating frequency in Figure 2(c) when the separation is 300 nm. Notice that one of the resonant frequencies (originally at 150 MHz) shifts to the left. This explained the enhancement of the friction torque for the single-layer structure at low-frequency range. This layered structure is favorable for the experiment since it gives a larger torque at lower rotating frequency. At this frequency, the mechanical rotor behaves more stable and hence easier for the measurement to be performed. We also show the dependence of thickness of

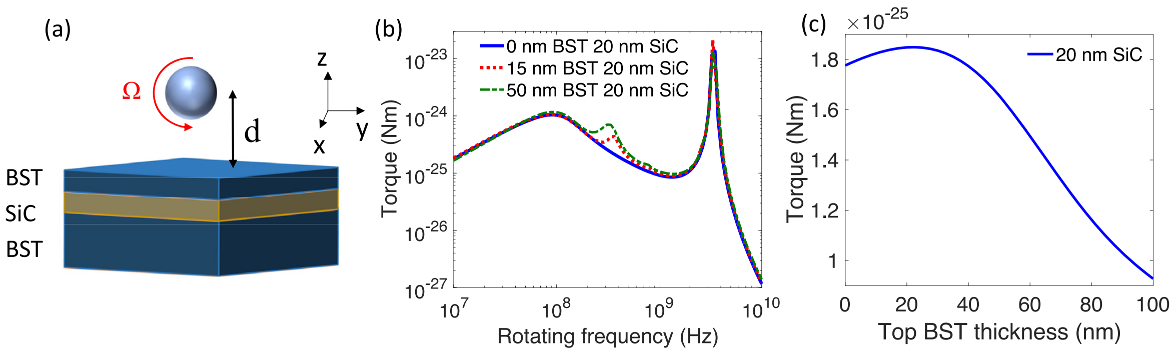

Figure 3: Vacuum friction between a barium strontium titanate (BST) sphere and a BST substrate with a double-layer coating on top. (a) A sphere with a radius of 75 nm rotates around the *x* axis, which is parallel to the plate. The plate consists of a thin layer of BST (shown in blue), a thin layer of SiC (shown in yellow) and a BST substrate. (b). Calculated vacuum frictional torque as a function of the rotating frequency of the nanosphere. The separation is 300 nm. The blue solid, red dashed, and green dashed curves correspond to a thin layer of 0-, 15-, and 50-nm BST on top of a 20-nm SiC-coated BST plate. (c). When the thickness of the second layer (SiC) is fixed to 20 nm and the rotating frequency is 10 MHz, the friction torque is shown as a function of the thickness of the first layer (BST). The separation is 300 nm.

the thin layer on the friction torque in Figure 2(d). It shows that 20-nm SiC, 20-nm Si_3N_4, and 60-nm SiO_2 give the largest friction torque. It is essential to find the optimum thickness of the coating to get the largest torque.

Beyond that, we also calculated the friction torque for the double-layer coating. The configuration is shown in Figure 3(a). The top is a thin layer of BST as shown in blue. The middle one is a 20-nm SiC thin layer similar to the former case and the bottom is a BST substrate. Similar to the single-layer coating, the transfer matrix for the $p(s)$ polarization is given as $T^{p(s)} = D_{0\to1}^{p(s)} P(L_1) D_{1\to2}^{p(s)} P(L_2) D_{2\to3}^{p(s)}$, where L_1 and L_2 is the thickness of the first and second layer coating, respectively. $D_{j\to j+1}^{p(s)}$ is the transmission matrix and $P(L_j)$ is the propagation matrix. At a separation of 300 nm, the calculated friction torque as a function of the rotating frequency is presented in Figure 3(b). The blue solid, red dashed, and green dashed curves corresponds to a thin layer of 0-, 15-, and 50-nm BST on top of a 20-nm SiC--coated BST plate. The torque for the double-layer is only slightly larger than the one with the single-layer coating at low-frequency range. Figure 3(c) shows the friction torque as a function of the thickness of the top BST layer when the rotating frequency is 10 MHz and the separation is 300 nm.

5 Conclusion

In this paper, we have calculated the vacuum friction between a rotating sphere and a close surface. We notice that BST has low surface phonon polariton frequency which can be mechanically excited. At two resonant rotating frequencies, the mechanical energy of the rotating sphere can be converted to the electromagnetic field energy and hence significantly enhance the vacuum friction torque. This provides us a more practical scheme to measure the long-sought vacuum friction torque. Moreover, we find that applying a single-layer coating on top of the BST substrate can further increase the friction torque by four times. The torque not only depends on the rotating frequency and the separation, but also relates to the thickness of the layer. The friction torque for the double-layer coating on the BST substrate is also presented in the content. In the future, it will be interesting to study whether more complex metamaterials [35] and topological materials [36] can further enhance the vacuum friction.

Acknowledgments: The authors are grateful to receive support from the DARPA QUEST program and the Office of Naval Research under Grant No. N00014-18-1-2371.
Author contribution: All the authors have accepted responsibility for the entire content of this submitted manuscript and approved submission.
Research funding: This research was supported by the DARPA QUEST program and the Office of Naval Research under Grant No. N00014-18-1-2371.
Conflict of interest statement: The authors declare no conflicts of interest regarding this article.

References

[1] H. B. G. Casimir, “On the attraction between two perfectly conducting plates,” *Proceedings*, vol. 51, pp. 793–795, 1948.
[2] J. B. Pendry, “Shearing the vacuum - quantum friction,” *J. Phys. Condens. Matter*, vol. 9, pp. 10301–10320, 1997.

[3] A. I. Volokitin and B. N. J. Persson, "Theory of friction: the contribution from a fluctuating electromagnetic field," *J. Phys. Condens. Matter*, vol. 11, pp. 345–359, 1999.

[4] P. A. Maia Neto and S. Reynaud, "Dissipative force on a sphere moving in vacuum," *Phys. Rev. A*, vol. 47, pp. 1639–1646, 1993.

[5] F. Intravaia, R. O. Behunin and D. A. R. Dalvit, "Quantum friction and fluctuation theorems," *Phys. Rev. A*, vol. 89, p. 050101, 2014.

[6] A. Manjavacas and F. J. García de Abajo, "Vacuum friction in rotating particles," *Phys. Rev. Lett.*, vol. 105, p. 113601, 2010.

[7] M. S. Tomassone and A. Widom, "Electronic friction forces on molecules moving near metals," *Phys. Rev. B*, vol. 56, pp. 4938–4943, 1997.

[8] A. I. Volokitin and B. N. J. Persson, "Resonant photon tunneling enhancement of the van der waals friction," *Phys. Rev. Lett.*, vol. 91, p. 106101, 2003.

[9] A. I. Volokitin and B. N. J. Persson, "Quantum friction," *Phys. Rev. Lett.*, vol. 106, p. 094502, 2011.

[10] R. Zhao, A. Manjavacas, F. J. García de Abajo, and J. B. Pendry, "Rotational quantum friction," *Phys. Rev. Lett.*, vol. 109, p. 123604, 2012.

[11] I. Dorofeyev, H. Fuchs, G. Wenning, and B. Gotsmann, "Brownian motion of microscopic solids under the action of fluctuating electromagnetic fields," *Phys. Rev. Lett.*, vol. 83, pp. 2402–2405, 1999.

[12] B. Gotsmann and H. Fuchs, "Dynamic force spectroscopy of conservative and dissipative forces in an al-au(111) tip-sample system," *Phys. Rev. Lett.*, vol. 86, pp. 2597–2600, 2001.

[13] B. C. Stipe, H. J. Mamin, T. D. Stowe, T. W. Kenny, and D. Rugar, "Noncontact friction and force fluctuations between closely spaced bodies," *Phys. Rev. Lett.*, vol. 87, p. 096801, 2001.

[14] G. Ranjit, M. Cunningham, K. Casey, and A. A. Geraci, "Zeptonewton force sensing with nanospheres in an optical lattice," *Phys. Rev. A*, vol. 93, p. 053801, 2016.

[15] Z. Xu and T. Li, "Detecting casimir torque with an optically levitated nanorod," *Phys. Rev. A*, vol. 96, p. 033843, 2017.

[16] J. Ahn, Z. Xu, J. Bang, et al., "Optically levitated nanodumbbell torsion balance and ghz nanomechanical rotor," *Phys. Rev. Lett.*, vol. 121, p. 033603, 2018.

[17] R. Reimann, M. Doderer, E. Hebestreit, et al., "Ghz rotation of an optically trapped nanoparticle in vacuum," *Phys. Rev. Lett.*, vol. 121, p. 033602, 2018.

[18] C. P. Blakemore, A. D. Rider, S. Roy, Q. Wang, A. Kawasaki, and G. Gratta, "Three-dimensional force-field microscopy with optically levitated microspheres," *Phys. Rev. A*, vol. 99, p. 023816, 2019.

[19] J. Ahn, Z. Xu, J. Bang, P. Ju, X. Gao, and T. Li, "Ultrasensitive torque detection with an optically levitated nanorotor," *Nat. Nanotechnol.*, vol. 15, pp. 89–93, 2020.

[20] Y. Zheng, L.-M. Zhou, Y. Dong, et al., "Robust optical-levitation-based metrology of nanoparticle's position and mass," *Phys. Rev. Lett.*, vol. 124, p. 223603, 2020.

[21] J. Bang, T. Seberson, P. Ju, et al., "5D Cooling and precession-coupled nonlinear dynamics of a levitated nanodumbbell," arXiv:2004.02384, 2020.

[22] R. Diehl, E. Hebestreit, R. Reimann, F. Tebbenjohanns, M. Frimmer, and L. Novotny, "Optical levitation and feedback cooling of a nanoparticle at subwavelength distances from a membrane," *Phys. Rev. A*, vol. 98, p. 013851, 2018.

[23] L. Magrini, R. A. Norte, R. Riedinger, et al., "Near-field coupling of a levitated nanoparticle to a photonic crystal cavity," *Optica*, vol.5, pp. 1597–1602, 2018.

[24] A. O. Turky, M. Mohamed Rashad, A. E.-H. Taha Kandil, and M. Bechelany, "Tuning the optical, electrical and magnetic properties of ba0.5sr0.5tixm1–xo3 (bst) nanopowders," *Phys. Chem. Chem. Phys.*, vol. 17, pp. 12553–12560, 2015.

[25] Y. Guo and Z. Jacob, "Giant non-equilibrium vacuum friction: role of singular evanescent wave resonances in moving media," *J. Opt.*, vol. 16, p. 114023, 2014.

[26] Y. Guo and Z. Jacob, "Singular evanescent wave resonances in moving media," *Opt. Express*, vol. 22, pp. 26193–26202, 2014.

[27] A. Volokitin, "Resonant photon emission during relative sliding of two dielectric plates," *Mod. Phys. Lett.*, vol. 35, p. 2040011, 2020.

[28] A. I. Volokitin, "Singular resonance in fluctuation-induced electromagnetic phenomena at the rotation of a nanoparticle near the surface of a condensed medium," *JETP Lett.*, vol. 108, pp. 147–154, 2018.

[29] J. Kischkat, S. Peters, B. Gruska, et al., "Mid-infrared optical properties of thin films of aluminum oxide, titanium dioxide, silicon dioxide, aluminum nitride, and silicon nitride," *Appl. Opt.*, vol. 51, pp. 6789–6798, 2012.

[30] J. Corson, G. W. Mulholland, and M. R. Zachariah, "Calculating the rotational friction coefficient of fractal aerosol particles in the transition regime using extended kirkwood-riseman theory," *Phys. Rev. E*, vol. 96, p. 013110, 2017.

[31] F. Tebbenjohanns, M. Frimmer, A. Militaru, V. Jain, and L. Novotny, "Cold damping of an optically levitated nanoparticle to microkelvin temperatures," *Phys. Rev. Lett.*, vol. 122, p. 223601, 2019.

[32] L. Ge, X. Shi, Z. Xu, and K. Gong, "Tunable casimir equilibria with phase change materials: from quantum trapping to its release," *Phys. Rev. B*, vol. 101, p. 104107, 2020.

[33] T. Zhan, X. Shi, Y. Dai, X. Liu, and J. Zi, "Transfer matrix method for optics in graphene layers," *J. Phys. Condens. Matter*, vol. 25, p. 215301, 2013.

[34] A. Manjavacas, F. J. Rodríguez-Fortuño, F. J. García de Abajo, and A. V. Zayats, "Lateral casimir force on a rotating particle near a planar surface," *Phys. Rev. Lett.*, vol. 118, p. 133605, 2017.

[35] X. Ni, Z. J. Wong, M. Mrejen, Y. Wang, and X. Zhang, "An ultrathin invisibility skin cloak for visible light," *Science*, vol. 349, p. 1310, 2015.

[36] Q.-D. Jiang and F. Wilczek, "Quantum atmospherics for materials diagnosis," *Phys. Rev. B*, vol. 99, p. 201104, 2020.